3. G. E. Schneider, *Brain Behav. Evol.* **8**, 73 (1973); D. O. Frost, *J. Comp. Neurol.* **203**, 227 (1981).
4. M. Sur *et al.*, *Science* **242**, 1437 (1988).
5. Four animals were mapped extensively and form the basis for this report. Procedures for preparing the animals for physiological recording were similar to those we have used previously (*4*). Animals were anesthetized with ketamine (30 mg of body weight per kilogram) and xylazine (2 mg/kg) and paralyzed with gallamine triethiodide (10 mg/kg per hour); their respiration was artificially controlled. Anesthesia was continuously monitored and maintained. End-tidal CO_2 was maintained at 4%. Parylene-insulated tungsten microelectrodes were used to record unit activity mostly in the middle layers of primary auditory cortex.
6. S. L. Pallas *et al.*, *J. Comp. Neurol.* **298**, 50 (1990).
7. We examined retinotopy and variability in the map in two ways. First, we plotted the azimuth of each receptive field against the mediolateral distance of the recording site from the medial edge of primary auditory cortex (and, separately, elevation against anteroposterior distance from the posterior edge of auditory cortex) and calculated a Pearson coefficient of correlation (r) along with the associated probability of departure from a random mapping. The coefficient of correlation was used because the variables under consideration, visual field azimuth (or elevation) and cortical distance, are essentially random samples from a bivariate distribution. Second, we defined a mapping index for azimuth (and separately for elevation) as the mean, over all recording sites, of |(actual value of receptive field azimuth − ideal value)|/(maximum value of azimuth represented − minimum value). We determined ideal azimuth and elevation values by overlaying isoazimuth and isoelevation lines over the mapped cortical region. The mapping index (for azimuth and elevation) would be 0 for a perfectly retinotopic map and close to 1 for a map without any topographic order.
8. For the map shown in Fig. 1, the mapping indices (±SEM) are 0.052 (±0.012) for azimuth and 0.124 (±0.055) for elevation.
9. Smoothed isoazimuth and isoelevation lines were fitted to the experimental data. Linear magnification factors, defined as the distance of cortex that represents a unit distance of visual field, were measured along a given isoelevation line as the extent of cortex representing each successive 10° of azimuth.
10. This is consistent with the demonstration that retinal W cells, which are distributed rather uniformly in the retina [D. J. Vitek, J. D. Schall, A. G. Leventhal, *J. Comp. Neurol.* **241**, 1 (1985); A. G. Leventhal, R. W. Rodieck, B. Dreher, *ibid.* **237**, 216 (1985)], provide the major input to the auditory pathway in lesioned ferrets [(*4*); A. W. Roe, P. E. Garraghty, M. Sur, *Soc. Neurosci. Abstr.* **13**, 1023 (1987); S. L. Pallas, J. Hahm, M. Sur, *ibid.* **15**, 495 (1989)]. In primary visual cortex of primates and carnivores [P. M. Daniel and D. Whitteridge, *J. Physiol. (London)* **159**, 203 (1961); R. Tusa, L. Palmer, A. Rosenquist, *J. Comp. Neurol.* **177**, 213 (1978); (*17*)], cortical magnification decreases approximately inversely with distance from central retina to the periphery, implying a logarithmic mapping of the retina on cortex.
11. Mapping indices for three other animals that were mapped extensively are (azimuth, elevation indices for each animal): 0.154 (±0.046), 0.252 (±0.079); 0.063 (±0.032), 0.278 (±0.101); 0.142 (±0.081), and 0.236 (±0.147). The correlation coefficients for the animals are (azimuth, elevation coefficient for each animal): 0.66, −0.39; 0.36, 0.35; and 0.95, 0.80. Magnification functions are very similar in different animals.
12. J. G. Kelly, P. W. Judge, D. P. Phillips, *Hear. Res.* **24**, 111 (1986).
13. Integrative properties appear to be represented along the isofrequency axis, such as discrete clusters of neurons related to EE or EI interactions between the two ears [T. J. Imig and J. Brugge, *J. Comp. Neurol.* **182**, 637 (1978); P. W. Judge and J. B. Kelly, *Soc. Neurosci. Abstr.* **14**, 651 (1988)] and the bandwidth of spectral tuning [M. L. Sutter and C. E. Schreiner, *ibid.* **15**, 1116 (1989)].
14. R. A. Andersen, P. L. Knight, M. M. Merzenich, *J. Comp. Neurol.* **194**, 663 (1980); S. Brandner and H. Redies, *J. Neurosci.* **10**, 50 (1990); (*15*). The pattern of projections from the auditory thalamus to auditory cortex in normal ferrets is very similar (*6*).
15. J. C. Middlebrooks and J. M. Zook, *J. Neurosci.* **3**, 203 (1983).
16. Our physiological mapping data (unpublished) suggest that retinal projections to the auditory thalamus are organized topographically. The projections from auditory thalamus to primary auditory cortex are as indicated in Fig. 2.
17. M. I. Law, K. R. Zahs, M. P. Stryker, *J. Comp. Neurol.* **278**, 157 (1988); A. W. Roe, S. L. Pallas, J.-O. Hahm, M. Sur, unpublished observations.
18. There are two ways by which thalamocortical projections can be widespread along the anteroposterior dimension of cortex in normal animals: (i) single thalamic cells have cortical arbors that are widespread along the anteroposterior dimension but restricted along the mediolateral dimension of cortex; and (ii) single thalamic cells have uniform cortical arbors, but cells close together have terminal fields that are widely dispersed along the anteroposterior dimension in cortex. It is possible that visual input alters either of these projection patterns in subtle ways in lesioned ferrets compared to normal ferrets.
19. D. N. Mastronarde, *J. Neurophysiol.* **49**, 303 (1983); D. Arnett and T. E. Spraker, *J. Physiol. (London)* **317**, 29 (1981); M. Meister, R. O. L. Wong, D. A. Baylor, C. J. Shatz, *Invest. Ophthalmol. Visual. Sci.* **31**, 115 (1990); L. Maffei and L. Galli-Resta, *Proc. Natl. Acad. Sci. U.S.A.* **87**, 2861 (1990).
20. We consider input selection to occur by a change in the weights of thalamocortical or intracortical synapses [M. Sur, S. L. Pallas, A. W. Roe, *Trends Neurosci.* **13**, 227 (1990)].
21. M. M. Merzenich, W. M. Jenkins, J. C. Middlebrooks, in *Dynamic Aspects of Neocortical Function*, G. M. Edelman, W. E. Gall, W. M. Cowan, Eds. (Wiley, New York, 1984), pp. 397–424.
22. Evidence from reorganization of maps after lesioning portions of peripheral input suggests that maps in both somatosensory cortex [M. M. Merzenich, G. Recanzone, W. M. Jenkins, T. T. Allard, R. J. Nudo, in *Neurobiology of Neocortex*, P. Rakic and W. Singer, Eds. (Wiley, New York, 1988), pp. 41–67] and visual cortex [J. H. Kaas *et al.*, *Science* **248**, 229 (1990)] are dynamically maintained.
23. We thank P. E. Garraghty for assisting in some experiments, T. Sullivan for assistance with histology, and P. Katz for comments on the manuscript. Supported by NIH grant EY07719 and by grants from the McKnight Foundation and the March of Dimes.

23 May 1990; accepted 10 September 1990

Analysis of Junctional Diversity During B Lymphocyte Development

KATHERYN MEEK

Immunoglobulin rearrangement is central to generating antibody diversity because of heterogeneity generated during recombination by deletion or addition of nucleotides at coding joints by the recombinase machinery. Examination of these junctional modifications revealed that the addition of nongermline-encoded nucleotides was more prevalent in adult versus fetal B cells, thus partially limiting the fetal antibody repertoire. In contrast, deletion of nucleotides occurs equivalently in B cells at different stages of development and at different points in B cell ontogeny. Finally, the bias in murine immunoglobulins for one D_H segment reading frame occurs at the D_HJ_H intermediate.

CRYSTAL STRUCTURES OF ANTIGEN-specific antibody molecules show that the hypervariable regions of the immunoglobulin heterodimer are integral to antigen binding (*1*)—thus variations in these regions engender different antigen specificities. Generally, the most variable portion is the third complementarity determining region (CDR3) (*2*).

The variation in CDR3 is generated by deletion of nucleotides from the coding sequences (presumably by an exonuclease associated with the recombinase machinery) and addition of nucleotides at the joints (N segments) in an apparently random fashion, probably by the enzyme terminal transferase (Tdt) (*3–9*). Though the rearrangement process is ostensibly random, in expressed immunoglobulins there is a preference for chains that have rearranged such that one particular D_H segment reading frame is used.

In this report, newborn and adult B cell receptors were examined for differences in junctional diversity. To analyze deletion of nucleotides from coding segments, I used the restriction enzyme sites that occur near the recombination signal sequences in various immunoglobulin gene segments (*10–14*). By digesting polymerase chain reaction (PCR)–amplified rearrangements with the appropriate restriction enzyme, the proportion of rearrangements that lacked that particular enzyme site was determined. Because in most situations the amplified rearrangements were not subject to antigenic selection (that is, D_HJ_H rearrangements or pseudogenes), the absence of the enzyme site should reflect the proportion of rearrangements that no longer contained the particular enzyme site because of nucleotide deletion during rearrangement.

Department of Internal Medicine, Division of Rheumatology, University of Texas Southwestern Medical Center, Dallas, TX 75235.

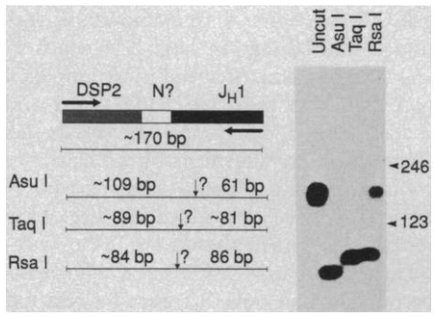

Fig. 1. (**Left**) Map of amplified DSP2 to J_H1 rearrangements. The black, white, and shaded boxes represent the J_H1 coding region, N region, and DSP2 coding region, respectively. Horizontal arrows depict the amplification primers. Positions of relevant restriction sites are indicated by the vertical arrows. Restriction sites that may or may not be present in an amplified rearrangement are followed by a question mark. Since the size of each rearrangement in the amplified pool of rearrangements will be variable depending on the degree of nucleotide deletion or addition, or both, the approximate lengths of the rearrangements have been indicated. Furthermore, after digestion with a particular enzyme, only one fragment will be of variable length; this has also been indicated. Sequences of relevant gene segments are from (*10*) and (*12*). Polymerase chain reactions were performed essentially as described previously (*23–25*). (**Right**) Southern hybridization experiment of DSP2 to J_H1 amplifications from adult spleen DNA, either uncut or restricted with indicated restriction endonucleases. The hybridization probe was an oligonucleotide complementary to the coding sequence of J_H1.

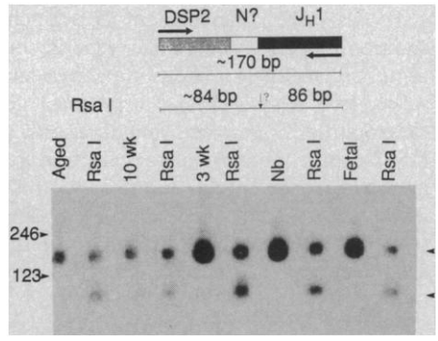

Fig. 2. (**Top**) Map of amplified DSP2 to J_H1 rearrangements. Positions of the Rsa I restriction site is indicated by the vertical arrow, as in Fig. 1. (**Bottom**) Southern hybridization of DSP2 to J_H1 amplifications from fetal, newborn, 3 week, 10 week, and adult spleen DNA, either uncut or digested with Rsa I. The hybridization probe was an oligonucleotide complementary to the 5′ flanking sequence of DSP2 D_H segments. The relative intensities of the hybridizing fragments were determined with a gel imager (Betascope, Betagen Inc., Waltham, Massachusetts). Position of the relevant fragments (uncut and 86 bp) are indicated with arrowheads.

DSP2 to J_H1 rearrangements from adult spleen DNA were amplified and then digested with three restriction endonucleases that cut within the J_H1 coding sequence (Fig. 1). Amplified DSP2-J_H1 rearrangements were digested with various restriction endonucleases and analyzed by Southern (DNA) blot hybridization with an oligonucleotide complementary to the J_H1 coding sequence. The Asu I site is the furthest from the site of recombination—29 nucleotides of J_H1 would have to be removed (considerably more than usually observed) to destroy the Asu I site. Thus, Asu I cuts the majority (if not all) of the amplified products and leaves a 61-bp fragment. Taq I sites, 12 nucleotides from the recombination site, are mostly intact. (Longer exposures show a small amount of product uncut by Taq I.) In contrast, many Rsa I sites, which are seven nucleotides from the recombination site, have been altered, leaving a significant amount of the product not digested (~170-bp fragment). This amount of nucleotide deletion is typical of immunoglobulin D_HJ_H rearrangement.

To analyze whether nucleotide deletion differs in adult versus fetal or newborn rearrangements, I amplified DSP2 to J_H1 rearrangements and assayed for the presence of the Rsa I site (Fig. 2). Both the uncut (~170 bp) and cut (86 bp) bands were present in D_HJ_H1 rearrangements from all ages, fetal to adult. By analyzing the intensities of the two bands, I determined that the destruction of the Rsa I site occurs at approximately the same frequency in B cell rearrangements from mice of all ages. Digestion with Taq I (site in J_H1) and Mae III (site in all DSP2 coding sequences) gave similar results (*15*). In addition, V_H to D_HJ_H rearrangements (V_H33, a J558 pseudogene to J_H3) digested with Rsa I (site in V_H33) gave similar results. Thus, the loss of nucleotides from coding sequences during immunoglobulin heavy chain recombination is roughly equivalent in newborn and adult rearrangements and is not differentially regulated through ontogeny.

$V_\kappa10$ to $J_\kappa1$ rearrangements were also analyzed for nucleotide deletion. The first nucleotide of the Mae II site is the fifth nucleotide of the $J_\kappa1$ coding sequence. There is a second Mae II site in the 3′ flanking region of the $J_\kappa1$ gene segment (Fig. 3).

After amplification and digestion with Mae II, a ^{32}P end-labeled oligonucleotide complementary to the third framework region was used as a hybridization probe. In both 10-week and newborn $V_\kappa J_\kappa$ rearrangements, the Mae II site is consistently absent in some rearrangements (represented by the presence of the 279-bp V_κ hybridizing fragment). Thus, these data show that the deletion mechanism affects all types of immunoglobulin recombination—rearrangements that occur early (heavy chain) and late (light chain) in lymphocyte differentiation and rearrangements from both newborn and adult lymphocytes. Hence, the enzyme responsible for nucleotide deletion is either an integral part of the recombinase machinery or its expression is coincident with that of the recombinase.

Lafaille *et al.* (*16*) have proposed that two nucleotides complementary to the last two bases of the coding sequences are added to the ends of the coding joints during recombination. These have been termed P nucleotides. Since P nucleotides form palindromes with adjacent coding sequences, their presence can be assayed with this system.

The P nucleotides that would be added to the 5′ end of the J_H2 gene segment create an Rsa I site and can be detected by amplifying DSP2 to J_H2 rearrangements and then cutting with Rsa I (Fig. 4). A DSP2 coding region probe detected a small portion of the amplified product with the predicted Rsa I site (78-bp band). P nucleotides at the 3′ end of all of the D_H segments and at the 5′ end of several J_H segments have been examined (*15*) and a small percentage of the amplified product is consistently digested with the predicted restriction endonuclease. This suggests that P nucleotides are added and maintained in a small fraction of rearrangements during the recombination process.

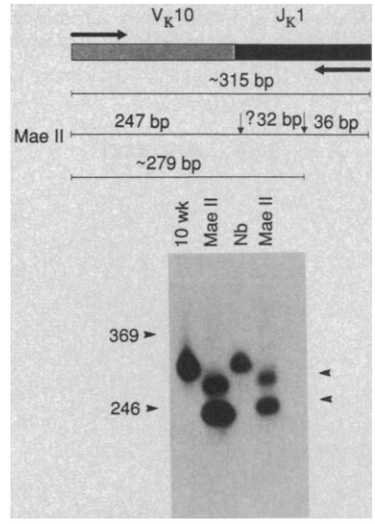

Fig. 3. (**Top**) Map of amplified $V_\kappa10$ to $J_\kappa1$ rearrangements (*11, 13*). The black and shaded boxes depict the $J_\kappa1$ and $V_\kappa1$ coding sequences, respectively. Positions of Mae II restriction sites are indicated by the vertical arrow as in Fig. 1. (**Bottom**) Southern hybridization experiment of amplifications from newborn and 10-week spleen DNA, either uncut or restricted with Mae II. Positions of the ~279-bp and 247-bp fragments are indicated with arrows. The hybridization probe was an oligonucleotide complementary to the third framework of $V_\kappa10$. The relative intensities of the hybridizing fragments were determined with a gel imager (Betascope, Betagen Inc.).

To assay for differences in N segment addition, I performed similar experiments using ^{32}P-labeled amplification primers and subsequent analysis by polyacrylamide gel electrophoresis. In these amplifications, a DSP2 coding sequence oligonucleotide was used to bias the amplification so that only joints that retained the entire DSP2 coding sequence were amplified. The size of the amplified rearrangements should be heterogeneous depending on the amount of deletion of the J_H segment and how much N segment addition occurred. The amplified products were restricted with Taq I and analyzed on a denaturing acrylamide gel (Fig. 5). In rearrangements in which the J_H coding sequence remains intact and no N nucleotides have been added, the size of the restricted fragment should be 28 bp (indicated with an arrow). Only rearrangements derived from animals that were 3 weeks old or older had any restricted fragments as large as (or larger than) 28 bp, evidence that N segment addition is minimal (if not totally absent) in fetal or newborn immunoglobulin rearrangements. This finding is consistent with sequence data from expressed immunoglobulins and T cell receptors from fetal and newborn animals (*16, 17*). However, the present study has the advantage of assaying N segment addition on a pool of rearrangements instead of clones. Also, since these experiments have been done on D_HJ_H intermediates (and not expressed immunoglobulins), this differential regulation is clearly not a result of antigen or repertoire selection.

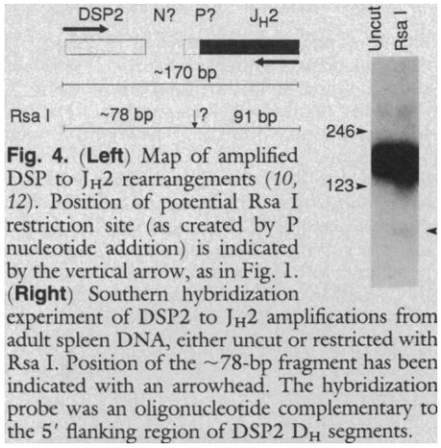

Fig. 4. (**Left**) Map of amplified DSP to J_H2 rearrangements (*10, 12*). Position of potential Rsa I restriction site (as created by P nucleotide addition) is indicated by the vertical arrow, as in Fig. 1. (**Right**) Southern hybridization experiment of DSP2 to J_H2 amplifications from adult spleen DNA, either uncut or restricted with Rsa I. Position of the ~78-bp fragment has been indicated with an arrowhead. The hybridization probe was an oligonucleotide complementary to the 5′ flanking region of DSP2 D_H segments.

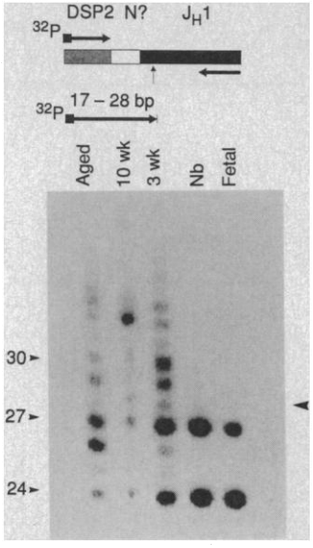

Fig. 5. (**Top**) Map of amplified DSP2 to J_H1 rearrangements with ^{32}P-labeled coding DSP2 oligonucleotide and unlabeled J_H1 oligonucleotide. Positions of Taq I restriction sites are indicated by the vertical arrow. The ^{32}P-labeled DSP2 coding oligonucleotide and the potential ^{32}P-labeled restriction fragments are indicated with horizontal arrows. If no nucleotides are deleted from J_H1 and no N segment nucleotides are present, the size of the labeled fragment will be 28 nucleotides. If all of the J_H segment up to the point of the Taq I site is deleted, the size of the labeled fragment will be 17 bp. (**Bottom**) Denaturing polyacrylamide gel electrophoresis of DSP2-J_H1 amplifications from fetal, newborn, 3-week, 10-week, and adult spleen DNA restricted with Taq I. Radiolabeled oligomers were used as molecular weight markers. The position of a 28-bp fragment is indicated with an arrowhead.

Furthermore, the restricted fragments (Fig. 5) are primarily in multiples of three nucleotides—an unanticipated result. Given that the D_HJ_H joints from newborn and fetal animals had no N segment additions, and that the entire DSP2 coding sequence was used (predicated by the amplification primer and conditions), the sequence of the predominant sized fragments can be deduced from their length. For example the 24-bp fragment must derive 16 bp from the DSP2 coding sequence and eight nucleotides from J_H1. Since Taq 1 cuts just after the 12th nucleotide of J_H1, four nucleotides from J_H1 must have been deleted during D_H to J_H recombination. Thus, the predominant fragments (24 bp and 27 bp) produce joints in which (with respect to J_H) the D_H segment is in the "preferred" D_H segment reading frame (*8*) or reading frame 3 (*2*). Similar experiments have been performed amplifying for other D_H to J_H rearrangements (with DFL16.1 and J_H2-4), and this bias for joints in which the D_H segment is in reading frame 3 is always apparent. In addition, the same phenomenon is observed in immunoglobulin D_HJ_H joints amplified from thymus DNA (*15*).

There are several potential explanations for this observation. It is feasible that there is a bias for D_HJ_H joints in a particular reading frame because of selection for $D_HJ_H\mu$ proteins (*18, 19*). However, all $D_HJ_H\mu$ proteins described thus far are from D_HJ_H joints in which the D_H segments are in reading frame 1 with respect to J_H; other D_HJ_H rearrangements are not translated (*18*). This suggests negative selection for $D_HJ_H\mu$ proteins. An alternative explanation for these results is that the bias for a particular D_H segment reading frame is a function of the recombinase machinery itself. One possible explanation for bias in the coding sequence ligation step of the recombination reaction is the presence of short sequence homologies at the ends of the two coding sequences. Short sequence homologies have been implicated in illegitimate recombination in eukaryotes in general (*20–22*). Gu *et al.* have suggested that short sequence homologies at the ends of the D_H and J_H gene segments bias immunoglobulin D_H to J_H joining (*17*). These data are consistent with that model.

REFERENCES AND NOTES

1. E. A. Padlan, D. D. Davies, S. Rudikoff, M. Potter, *Immunochemistry* **13**, 945 (1981).
2. E. A. Kabat, T. T. Wu, M. Reid-Miller, H. M. Perry, K. S. Gottesman, *Sequences of Proteins of Immunologic Interest* (Department of Health and Human Services, Bethesda, MD, ed. 4, 1987).
3. S. V. Desiderio *et al.*, *Nature* **311**, 752 (1984).
4. T. Honjo, *Annu. Rev. Immunol.* **1**, 499 (1983).
5. S. Tonegawa, *Nature* **302**, 575 (1983).
6. S. Lewis, A. Gifford, D. Baltimore, *Science* **228**, 677 (1985).
7. S. V. Desiderio and K. R. Wolff, *J. Exp. Med.* **167**, 372 (1988).
8. M. Kaartinen and O. Makela, *Immunol. Today* **6**, 324 (1985).
9. F. W. Alt and D. Baltimore, *Proc. Natl. Acad. Sci. U.S.A.* **79**, 4118 (1982).
10. Y. Kurosawa and S. Tonegawa, *J. Exp. Med.* **155**, 201 (1982).
11. H. Sakano, K. Huppi, G. Heinrich, S. Tonegawa, *Nature* **280**, 288 (1979).
12. C. Wood and S. Tonegawa, *Proc. Natl. Acad. Sci. U.S.A.* **80**, 3034 (1983).
13. I. Sanz and J. D. Capra, *ibid.* **84**, 1085 (1987).
14. A. L. M. Bothwell *et al.*, *Cell* **24**, 625 (1981).
15. K. Meek, unpublished data.
16. J. J. Lafaille, A. DeCloux, M. Bonneville, Y. Takagake, S. Tonegawa, *Cell* **59**, 859 (1989).
17. H. Gu, I. Forster, K. Rajewsky, *EMBO J.* **9**, 2133 (1990).
18. M. G. Reth and F. W. Alt, *Nature* **312**, 418 (1984).
19. M. Reth, E. Petrac, P. Wiese, L. Lobel, F. W. Alt, *EMBO J.* **11**, 3299 (1987).
20. D. B. Roth and J. H. Wilson, *Mol. Cell. Biol.* **6**, 4295 (1986).
21. P. Pfeiffer and W. Vielmetter, *Nucleic Acids Res.* **16**, 907 (1988).
22. S. Thode, A. Schafer, P. Pfeiffer, W. Vielmetter, *Cell* **60**, 921 (1990).
23. R. K. Saiki *et al.*, *Science* **230**, 1350 (1985).
24. K. D. Meek, C. A. Hasemann, J. D. Capra, *J. Exp. Med.* **170**, 39 (1989).
25. Under the amplification conditions I used, the DSP2 oligonucleotide amplifies all DSP2 D_H segments, but not DQ52 or DFL16 D_H segments. The J_H1 oligonucleotide amplifies only the J_H1 gene segment. Furthermore, this combination of oligonucleotides does not amplify the unrearranged configuration because the most J_H proximal DSP2 D_H segments is approximately 18 kb from J_H1. Amplified DNA was digested with an excess amount of each restriction endonuclease. Puc18 DNA (0.5 μg) was included as an internal control for complete digestion. Southern hybridization was done as described previously (*24*). To ensure that PCR artifacts did not interfere with the interpretation of these experiments, I included controls with no DNA to each experiment, and each experiment (Figs. 1 to 5) was repeated several times with consistent results. Finally, to ascertain how often a particular site might

be generated via random chance in the N segment, DSP2 to J_H3 rearrangements (which lack RSA I sites) were amplified and digested with Rsa I and no cutting could be detected.

26. I am grateful to C. Hasemann, L. Van Dyk, J. D. Capra, R. Baer, and P. Lipsky for helpful discussions and comments on the manuscript. This work was supported by the Arthritis Foundation.

29 June 1990; accepted 21 September 1990

A Mouse Model of the Aniridia-Wilms Tumor Deletion Syndrome

TOM GLASER,* JOAN LANE, DAVID HOUSMAN

Deletion of chromosome 11p13 in humans produces the WAGR syndrome, consisting of aniridia (an absence or malformation of the iris), Wilms tumor (nephroblastoma), genitourinary malformations, and mental retardation. An interspecies backcross between *Mus musculus/domesticus* and *Mus spretus* was made in order to map the homologous chromosomal region in the mouse genome and to define an animal model of this syndrome. Nine evolutionarily conserved DNA clones from proximal human 11p were localized on mouse chromosome 2 near *Small-eyes* (*Sey*), a semidominant mutation that is phenotypically similar to aniridia. Analysis of Dickie's Small-eye (Sey^{Dey}), a poorly viable allele that has pleiotropic effects, revealed the deletion of three clones, *f3*, *f8*, and *k13*, which encompass the aniridia (*AN2*) and Wilms tumor susceptibility genes in man. Unlike their human counterparts, Sey^{Dey}/+ mice do not develop nephroblastomas. These findings suggest that the Small-eye defect is genetically equivalent to human aniridia, but that loss of the murine homolog of the Wilms tumor gene is not sufficient for tumor initiation. A comparison among *Sey* alleles suggests that the *AN2* gene product is required for induction of the lens and nasal placodes.

THE EYE HAS LONG PROVIDED A system for studying inductive interactions during embryonic development. In vertebrates, considerable insight into eye development has been gained through classical ablation and transplantation experiments, yet little is known about the underlying molecular events (*1*). In *Drosophila*, a key to understanding the morphogenesis of the compound eye has been the identification of mutations that affect various stages of eye development (*2*). A potentially comparable mutation in humans results in aniridia, an autosomal dominant disorder in which the iris is absent or malformed (*3*). It can occur as an isolated abnormality, affecting one in 60,000 people, or together with Wilms tumor in 25 to 33% of cases, as part of the WAGR $11p^-$ deletion syndrome (*4*). The phenotype varies from a nearly complete absence of iris tissue to a subtle thinning of the iris margin in an otherwise normal eye. Vision is often impaired because of concomitant hypoplasia of the fovea and optic nerve, and commonly deteriorates over a period of years as a result of cataracts, glaucoma, and corneal opacification (*3*). An aniridia gene (*AN2*) has been mapped within chromosome band 11p13 by analysis of overlapping WAGR deletions, reciprocal translocations in two aniridia families, and meiotic linkage in aniridia pedigrees (*5*). *AN2* forms part of the WAGR gene complex and is telomeric to the Wilms tumor susceptibility locus (*WT1*). We have isolated a set of recombinant DNA clones that are densely distributed throughout this region (*6*). We have now used these probes in a comparative mapping approach to define a mouse model for the WAGR syndrome.

The WAGR complex is flanked by genes that encode catalase (*CAT*) and the β chain of follicle-stimulating hormone (*FSHB*) (*5*), which are located on chromosome 2 in the mouse genome and are there denoted as *Cas-1* and *Fshb*, respectively (*7*). To map this region more precisely, we selected nine probes from the proximal short arm of human chromosome 11 that cross-hybridize with rodent DNA (Table 1). Probes *g2*, *f3*, *k13*, *f8*, and *o3* were derived from an irradiation-reduced somatic cell hybrid that contained a 3000-kilobase (kb) segment of band 11p13 as its only human DNA (*8*). The probes are interspersed within the WAGR complex and detect three transcribed genes (*6*), including one that has been directly implicated in Wilms tumorigenesis (*9, 10*). The gene order has been established by deletion analysis as follows (*5, 6*): *D11S14-CAT-g2-f3-(WT1, k13, f8)-AN2-o3-D11S16-FSHB*-11pter. Under conditions of reduced hybridization stringency, each probe detects a set of restriction fragment variants between *Mus musculus/domesticus* (the laboratory mouse) and *Mus spretus* (the western Mediterranean short-tailed mouse) (*11*). These restriction fragment variants were used to score a panel of 94 interspecies backcross mice (Fig. 1A). The nine probes from human chromosome 11p cosegregated in the center of mouse chromosome 2, between *ld*, a gene controlling limb development (*12*), and the glucagon gene (*Gcg*) (Fig. 1B). All other potential orders required several double and triple crossovers (Table 2). These results and similar multipoint linkage data of others (*13*) strongly suggest that *Cas-1* is not distal to the gene for β_2 microglobulin (*B2m*), as it appears in the consensus map (*14*). Furthermore, the results localized the murine WAGR region close to the semidominant mutation Small-eyes (*Sey*), the phenotype and inheritance pattern of which resemble human aniridia (*15*).

Individuals with aniridia and *Sey*/+ mice have similarly malformed eyes. Both suffer from a complete or partial absence of iris tissue, although the phenotype in each species varies considerably among carriers of the same mutant allele. In general, the ocular defects in *Sey*/+ mice are more extreme. In most cases, the eyes are less than half their normal size (microphthalmos), the anterior chamber of the eye is missing, the retina is abnormally folded, and the lens is absent or small and has anterior cataracts (*15*).

The *Sey* gene has been mapped in multipoint crosses 5 centimorgans (cM) proximal to *pallid* (*pa*), a region corresponding to Giemsa bands 2D or 2E (*15, 16*). Three mutant alleles have been described (*15*). The most deleterious are Sey^{Dey}, a spontaneous variant, and Sey^{H}, a mutation induced by x-irradiation of oocytes. Carriers of these alleles also have a white belly spot, have reduced pigmentation of their tails and feet, and are 10 to 20% smaller than their wild-type littermates. Fetal loss among heterozygotes is about 60%, and homozygous embryos die on or before the 6th day of gestation. The third allele, Sey^{MH}, produces defects in heterozygotes that are limited to the eye. Homozygous Sey^{MH}/Sey^{MH} embryos survive to birth but lack eyes and noses. On the basis of these findings, it has been proposed that Sey^{Dey} and Sey^{H} result from large deletions but that Sey^{MH} is an intragenic deletion or point mutation (*15*).

To investigate the relation between Small-

T. Glaser, Center for Cancer Research, Massachusetts Institute of Technology, Cambridge, MA 02139, and Harvard Medical School, Boston, MA 02115.
J. Lane and D. Housman, Center for Cancer Research, Massachusetts Institute of Technology, Cambridge, MA 02139.

*To whom correspondence should be addressed.